Article

Growth Kinetic Parameters and Prediction of Growth and Zearalenone and Deoxynivalenol Production Boundaries by Three *Fusarium asiaticum* Strains Isolated from Wheat

Esther Garcia-Cela [1,2,*], Carol Verheecke-Vaessen [1], Inga Ósk-Jónsdóttir [1], Rita Lawson [1,2] and Naresh Magan [1]

1   Applied Mycology Group, Environment AgriFood Theme, Cranfield University, Cranfield MK43 0AL, UK
2   Clinical, Pharmaceutical and Biological Sciences, School of Life and Medical Sciences, University of Hertfordshire, Hatfield AL10 9AB, UK
*   Correspondence: e.garcia-cela@herts.ac.uk

Abstract: *Fusarium* species can cause head blight of cereals worldwide. This is accompanied by impacts on yield and contamination of grains with mycotoxins. Regulations, with maximum limits, exist for the relevant *Fusarium* mycotoxins (e.g., type A and B trichothecenes, zearalenone and fumonisins). There is interest in a better understanding of the effect of key interacting abiotic factors which determine colonization and mycotoxin production in small grain cereals. Thus, this study examined the ecophysiological relationship between temperature and water availability (10–35 °C; water activity, a_w, 0.87–0.98) on growth and production of *Fusarium* mycotoxins (zearelenone, ZEA; deoxynivalenol, DON; 3-acetyl deoxynivalenol, 3-Ac-DON and nivalenol, NIV) by three strains of *F. asiaticum*, a head blight pathogen isolated from China and becoming important in other global regions. These were carried out on simulated wheat-based matrices that identified the optimum (25 °C/0.98 a_w) and marginal boundary conditions for growth (35 °C/0.90 a_w) for all three strains. Contrarily, different mycotoxigenic profiles were observed between strains ($p < 0.05$). Four mycotoxins assessed were produced at 30 °C while cold temperature inhibited the production of NIV and ZEA, which were never detected at <20 and <15 °C, respectively. Optimal mycotoxin production conditions varied for each toxin with ZEA production which was best at 30 °C/0.93–0.95 a_w, DON, 3-Ac-DON and NIV which was 0.98 a_w/20–30 °C. Probabilistic models were used to predict growth and regulated mycotoxin production by the strains of *F. asiaticum*. This study will be beneficial in the development mitigation strategies for control of pre- and post-harvest colonization of cereals and mycotoxin contamination by this *Fusarium* species in cereals.

Keywords: predictive model; probabilistic model; wheat; barley; trichothecenes; zearalenone; deoxynivalenol

1. Introduction

Wheat is a cereal harvested from different species belonging to the *Triticum* genera, cultivated worldwide but originally from the Mediterranean and West Asia regions. The global production of this cereal reached the 762M tonnes in 2020 [1]. After harvesting, inefficient drying of wheat grain can result in rapid deterioration during subsequent post-harvest storage phases [2]. The contamination with mycotoxins has economic and trade implications, especially if not meeting the relevant legislative maximum limits as well as health risk implications. It has been suggested that approx. 18% of wheat production is lost due to fungal invasion [3]. Fusarium head blight (FHB) of wheat, caused mainly by a few members of the *Fusarium graminearum* species complex (FGSC), is a major threat to agricultural grain production, food safety, and animal health [4]. Currently, the complex includes at least 15 distinct species (*F. acaciae-mearnsii, F. asiaticum, F. aethiopicum, F. austroamericanum, F. boothii, F. brasilicum, F. cortaderiae, F. gerlachii, F. graminearum, F. louisianense,*

F. meridionale, F. mesoamericanum, F. nepalense, F. ussurianum, F. vorosii) that vary in aggressiveness, growth rate, and geographical distribution but lack morphological differentiation [5]. Diversity in metabolic capabilities within the complex, including toxin metabolites such as trichothecenes type B and their variant forms (Deoxynivalenol (DON), Nivalenol (NIV), 3-acetyl-deoxynivalenol (3-DON), 15-acetyl-deoxynivalenol (15-DON)) and Zearalenone (ZEA) have been observed among species in the complex [6,7]. In addition, trichothecenes exposure can cause feed refusal, immunological problems, vomiting, skin dermatitis, and hemorrhagic lesions, while ZEA exposure causes hyperplasia and infertility [8].

Once cereals are harvested, they are dried and stored directly or transported to central silos for short to medium term storage prior to processing [9]. Depending on final use, minimizing mould spoilage and mycotoxin contamination can be achieved using modified atmosphere storage, chemical preservation systems, biocontrol agents or monitoring systems for temperature and equilibrium relative humidity or intergranular CO_2 linked to postharvest risk models [2]. Some of these approaches have been effective in reducing fungal contamination and mycotoxin production in laboratory or pilot scale systems, and transference to industry depends on the cost-benefit analyses.

The two most important abiotic factors determining fungal colonization and mycotoxin production by fungi are water activity (a_w) and temperature (T) [10]. Knowledge of the optimum and marginal conditions of $a_w \times$ temperature for different mycotoxigenic fungi is critical in understanding the relative risks of spoilage and toxin contamination. At present, T and sometimes relative humidity (RH) sensors are being used in silos and during transport to monitor these two key parameters in stored cereals. Species-specific models of ecophysiological conditions for optimum, and especially marginal conditions for growth/mycotoxin production, could be effectively utilized in conjunction with real-time sensor systems for these abiotic parameters can be beneficial in supporting and improving post-harvest management decisions and reducing food spoilage.

A number of studies have used both primary and secondary kinetic and probabilistic models for predicting both fungal growth and mycotoxin production, especially by xerophilic *Aspergillus* species [11–14] as well as some *Fusarium* species [15–18]. In most studies, authors model the fungal growth based on the radial growth of a fungal spore inoculated in the centre of the media containing the matrix-based media or the actual matrix. In contrast, Pei [18] used the same mathematical approach, but they modelled the number of colony-forming units (CFUs) instead of the radial growth. However, much less is known about the ecology of *F. asiaticum* [19,20]. This is an emergent pathogen within the FGSC, which is relatively indistinguishable from *F. graminearum,* which was found to be predominant in China. It has also become important in other southern Asian regions and has been reported to be present on cereals in Brazil, Japan, Nepal, and USA [21–25]. It is a predominant species responsible for FHB in southern China or where temperature and rainfall are above 22 °C and 320 mm, respectively [26]. However, there is a lack of information on the ecophysiology of strains of this species. This is critical to the development of effective strategies for their control to minimize effects on crop yield/quality and on mycotoxin contamination.

The objectives of this study were to (a) examine the effects of two-way interacting abiotic factors of $a_w \times$ T on growth of the strains of *F. asiaticum* and (b) on DON and ZEA production, and (c) utilize this information to develop mathematical models for both growth and mycotoxin production (ZEA/DON) as a function of the two-way interacting abiotic factors.

2. Materials and Methods

2.1. Fungal Strains and Experimental Design

In this study, three strains of *F. asiaticum* were used. The strains were isolated in China from 2002–2005 in three different regions and from different hosts, as shown in Table 1.

Table 1. Information about *F. asiaticum* strains included in this study.

Species	Isolate Code	Year	Region	Host	Latitude
F. asiaticum	CH024b	2002	Wuhan	Wheat	N/A
F. asiaticum	bfb0082_1	2005	Wuchang	Barley	114°07′
F. asiaticum	bfb0982_1	2005	Xingsheng, Sichuan	Barley	105°02′

N/A: not available.

A full factorial experimental design including five different a_w levels (0.98, 0.95, 0.93, 0.90, and 0.87) and six different temperatures (10, 15, 20, 25, 30 and 35 °C) for 10 days were performed. Four replicates were used for each of the conditions. Zearalenone (ZEA) and Deoxynivalenol (DON), 3-acetylDON (3Ac-DON), 15-acetyl DON (15-Ac-DON) and Nivalenol (NIV) were quantified at the end of the incubation periods.

2.2. Ecophysiological Study

2.2.1. Media Preparation and Inoculation

The basal wheat-based media (3% milled wheat + 1.5% agar) was modified to 0.98, 0.95, 0.93, 0.90, and 0.87 a_w. This was done by making up non-ionic solute mixtures of water/glycerol solutions which contained 9.8, 25.5, 36.0, 51.8, and 67.5 g of glycerol per 100 mL, respectively. These were thoroughly mixed and 100 mL of the mixture was used for making the different a_w treatments. The media was autoclaved at 121 °C in a bench top autoclave and the molten media poured (approx. 17.5 mL) into 9 cm sterile Petri plates in a sterile flow bench. The final a_w was checked with an AquaLab Series 4 TE (Decagon Devices, Inc., Washington, USA) and found to be within ± 0.003 of target values.

To obtain heavily sporulating cultures for wheat-based media inoculation, all strains were inoculated onto V8 agar (V8®, 175 mL; 3 g; $ZnSO_4 \cdot 7H_2O$, 0.01 g; $CuSO_4 \cdot 5H_2O$, 0.005 g; agar, 20 g/L) Petri plates and incubated at 25 °C in darkness for 10 days. To make a spore suspension, sterile water containing Tween 80 (0.005%) was added to the colony and rubbed with a surface-sterilized spatula by gently brushing the surface. After thorough mixing, a Thoma counting chamber was used to de oftermine the number of spores/mL and the concentration adjusted to 1×10^5 spores/mL. Finally, 5 µL were used to centrally inoculate the different treatment and replicate wheat-based media. Media of the same aw were kept separately in sealed bags at each temperature. The colony diameters of each replicate and treatment were measured daily in two directions at right angles to each other for 10 days or until the colony reached the edge of the 9 cm Petri plate.

2.2.2. Kinect Model

A two-step modelling approach, including primary and secondary modelling, was employed to quantify the effect of temperature (T) and water activity (a_w) on the kinetic parameters of the three strains of *F. asiaticum*. Initially, estimates of the growth rates of the strains were obtained by plotting the colony diameters against time. For each treatment, a non-linear regression was applied to estimate the maximum growth rate (µmax, mm/day), lag phase prior to growth (λ, day), and maximum colony diameter, if applicable, by fitting the experimental data to the primary model of Baranyi and Roberts (1997) [11] (Equation (1)) by using Statgraphics 18® Centurion (Manugistics Inc.: Rockville, MD, USA). Following the approach used previously by [27].

$$Colony\ diameter = \mu_{max}A - ln\left\{1 + \frac{[exp(\mu_{max}A)] - 1}{exp(D_{max})}\right\} \tag{1}$$

$$A = t + \left(\frac{1}{\mu_{max}}\right) + ln[exp(-\mu_{max}t) + exp(-\mu_{max}\lambda) - exp(-\mu_{max}t - \mu_{max}\lambda)]$$

where: D_{max}: maximum colony diameter; t: time

The estimates of μmax were further fitted to the gamma/concept [28], and combined secondary models were proposed by [29,30] by multivariable regression to describe the effect of temperature and aw on fungal growth rate. The model is described in Equation (2).

$$\mu_{max}(T, a_w) = \mu_{opt} \cdot \tau(T) \cdot \rho(a_w) \tag{2}$$

where

$$\tau(T) = \left(\frac{(T - T_{min})^2 \cdot (T - T_{max})}{(T_{opt} - T_{min}) \cdot \left[(T_{opt} - T_{min})(T - T_{opt}) - (T_{opt} - T_{max})(T_{opt} + T_{min} - 2T) \right]} \right)$$

$$\rho(a_w) = \left(\frac{(a_w - a_{wmin})^2 \cdot (a_w - a_{wmax})}{(a_{wopt} - a_{wmin}) \cdot \left[(a_{wopt} - a_{wmin})(a_w - a_{wopt}) - (a_{wopt} - a_{wmax})(a_{wopt} + a_{wmin} - 2a_w) \right]} \right)$$

where:

T_{min} is the temperature below which growth is no longer observed.
T_{max} is the temperature above which no growth occurs.
T_{opt} is the temperature at which maximum growth rate equals its optimal value μ_{opt}.
a_{wmin} is the aw below which growth is no longer observed.
a_{wmax} is the aw above which no growth occurs.
a_{wopt} is the a_w at which maximum growth rate equals its optimal value μ_{opt}.

The non-linear regression option in Statgraphics 18® Centurion (Manugistics, Inc., Rockville, MD, USA) was used to fit the multifactorial secondary models to the data. Homogeneity of variance of the untransformed dependent variable was checked by determining the correlation between the mean growth rate and the variance of the three isolates at different temperatures and aw levels. Untransformed μ_{max} data were uncorrelated to the variance, and data were used with no further transformation of growth rate data following the approach used previously by [13].

2.2.3. Modelling of the Growth/no Growth and Toxin/no Toxin Production Interface

Logistic regression in Statgraphics 18® Centurion (Manugistics Inc.: Rockville, MD, USA) was used to analyze the probabilities of growth and mycotoxin production according to temperature and aw. Backward stepwise factor selection was used to choose the final model according to the relative significant factors ($p < 0.05$). Experimental data for growth and toxin production were transformed into the binary values: 0 for the absence of growth/production and 1 for growth/production. To estimate the probabilities of growth/production, the experimental data were fitted into a logistic regression model previously described [14]. A probabilistic model (Equation (3)) was used to predict the probabilities for growth of *F. asiaticum*, while another model (Equation (4)) was used to predict the probabilities of production of DON and ZEA which are both regulated mycotoxins in the EU.

$$LogitP = ln\left(\frac{P}{1 - P} \right) = b_0 + b_1 T + b_{11} T^2 + b_{12} a_w T + b_2 a_w^2 + b_{22} a_w + b_3 time \tag{3}$$

$$LogitP = ln\left(\frac{P}{1 - P} \right) = b_0 + b_1 T + b_{11} T^2 + b_{12} a_w T + b_2 a_w^2 + b_{22} a_w \tag{4}$$

p: probability of growth/toxin production.
b_i: the coefficients to be estimated.
The prediction of boundaries for 10, 50, and 90% probability of growth/production was calculated using Microsoft® Excel® for Microsoft 365 MSO (Version 2208).

2.3. Mycotoxin Analysis

2.3.1. Mycotoxin Extraction from Agar

At the end of the incubation period (10 days), the colony and agar were cut in half with a surface sterilized scalpel and carefully placed in a previously weighed 50 mL Falcon tube. These samples were immediately frozen at −20 °C for subsequent mycotoxin extraction and analysis.

Samples were then thawed and ground with a spatula for 1 min. Approximately a threefold sample weight of extraction solvent (Acetonitrile: formic acid: water (79:20.9:0.1 $v/v/v$)) was added. The mixture was vortexed on a rotary shaker in the dark at 300 rpm at 25 °C for 90 min on a Stuart Orbital shaker SSL1. Following this shaking period, the tubes were centrifuged at 3800 rpm for 10 min (Thermo Scientific Sorvall ST40 Centrifuge, Loughborough, UK) and the supernatant was transferred to new 50 mL Falcon tubes. A 0.5 mL aliquot of the supernatant was transferred with a syringe and filtered into 2 mL chromatography silanized amber vials and stored at −20 °C until analysis using LC-MS/MS.

2.3.2. Mycotoxin Analysis

An Exion series ultrahigh performance liquid chromatography system coupled to 6500+ qTRAP-MS-MS system coupled with IonDrice TM Turbo Spray (Sciex Technologies, Warrington, UK) was used to perform the mycotoxins quantification. The column was ACE 3-C18/2.1 × 100 mm, 3 μm particle size; Hichrom, Reading, UK) equipped with a C18 security guard cartridge (4 × 3 mm, Gemini Agilent) and kept at 40 °C. The gradient elution was carried out with two mobile phases, water: acetic acid (99:1 v/v) (solvent A) and methanol: acetic acid (99:1 v/v) (solvent B) as follows: 0.0–2.0 min: 10–40% B; 2.0–10.0 min: 100% B; 11.50–12.0 min: 100–10% B; 12.00–15.0 min: 10% B. Both solvents included 5 mM ammonium acetate to promote ammonium adducts. The flow rate was 0.3 mL/min, and the injection volume was set to 1μL.

An unscheduled Multiple Reaction Monitoring (MRM) mode was used to perform ESI-MS/MS in positive and negative mode, dwell time 10 msec per Q3 analyzed. The source conditions were set as described: Curtain gas 40%, Collision Gas Medium, IonSpray voltage in negative: −4500 V and in positive: 5500 V, Temperature 400 °C, ion source gas 1: 60 psi and ion source gas 2: 60 psi, 10 V was fixed for all compounds in Entrance Potential. Confirming the identity of the identified metabolite was performed through the use of 2 MRM per analyte and further analyzed with Analyst® Data Asquisition version 1.6.3, and quantification of data was performed with MultiQuant® version 3.0.3 as described in [31] Isidro-sanchez et al. (2020) and described in Supplementary Table S1.

2.3.3. Mycotoxin Analysis Performance

Wheat-based media were spiked prior to solidification. Spiking solutions contained all the target analytes in acetonitrile at five concentrations (10, 50, 250, 500, 1000 ng/g) and vortexed. The vials were left open for approximately 2 h to obtain an equilibrium between the analytes and the matrix and to allow solvent evaporation. The vials were kept overnight at −20 °C, and the day after each vial was thawed, homogenized with a spatula and 200 ± 10 mg divided into eight new vials. These were extracted as described in Section 2.3.1. A total of 200 μL were transferred to silanized amber vials, and four replicates out of eight were spiked again after extraction to the same concentration as before. These were then kept at −20 °C, thawed and analyzed as described in Section 2.3.2. The peaks were integrated, linear 1/x weighted, calibration curves were built and the data were corrected based on the recovery obtained. The recovery and Limit of detection (LOD) and Limit of Quantification (LOQ) were calculated as described in [32] and listed in Supplementary Table S1.

2.4. Statistical Analysis

Statistical analysis was conducted using JMP Pro 14.0 and Statgraphics 18® Centurion (Manugistics Inc.: Rockville, MD, USA) Every dataset was tested for normality, and homoscedasticity was checked with Levene's value, but the data never fulfilled the requirements for parametric test. Therefore, the non-parametric Wilcoxon test was performed to test for significant difference between environmental factors and strains regarding ecophysiology and mycotoxin production with probability, p = 95% (p-value: ≤ 0.05). Comparisons for each pair using the Wilcoxon method was used to detect where the difference/no difference occurred. Statistical analysis was only conducted on conditions where growth/mycotoxin production occurred during the 10 days incubation period. All values for mycotoxin production between LOD and LOQ or above LOQ were included in the statistical analysis and in the case where no mycotoxin was formed, zero values were transformed into half LOD.

3. Results

3.1. Ecophysiological Study Fungal Growth

3.1.1. Kinetic Primary Model

The diametric growth rate increased in a linear fashion with both aw and T (Figure 1). The maximum growth rate (μ_{max}) and lag phase (λ) prior to growth of the *F. asiatiacum* strains on the wheat-based media were estimated by the biphasic Baranyi's function (see Figure 1, Table 2). No significant differences in these parameters were found between the three strains ($p > 0.05$). However, aw and T significantly affected both parameters ($p < 0.05$). The more available water, the shorter the lag phase prior to growth was and the maximum growth rate was increased. The only exception was 20 °C/0.95 a_w for the three strains. Growth was observed at 10 °C, although only at the highest aw levels tested (0.95, 0.98). However, when the temperature was optimal (20–30 °C), growth occurred with less available water (e.g., 0.90–0.93 a_w). Under extreme temperature stress such as 35 °C, no growth occurred at 0.90 a_w. Maximum fungal growth was always observed at 25 °C (Figure 2).
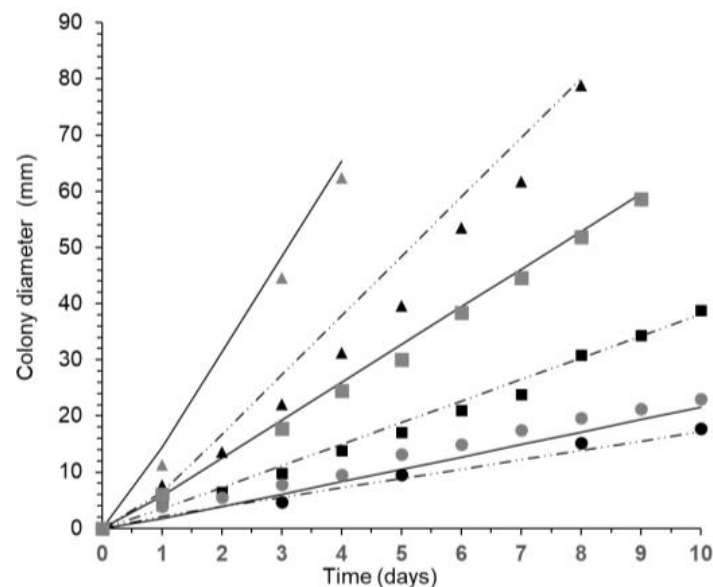

Figure 1. Fitted colony growth curves for *F. asiaticum* (strain 082) on wheat-based media at 35 °C (▲, 0.98 a_w; ■, 0.95 a_w; ●, 0.93 a_w) and 25 °C (▲, 0.98 a_w; ■, 0.95 a_w; ●, 0.93 a_w) fitted to Baranyi model (–, 30 °C, ·····, 15°C).

Table 2. Estimated maximum growth rate (μ_{max}) and lag phase (λ, days) of *F. asiatiacum* on wheat-based media under different $a_w \times T$ conditions.

T (°C)	a_w	*F. asiaticum* -982		*F. asiaticum* -082		*F. asiaticum* -Ch024b	
		λ (day) $\pm$ SD	μ_{max} (mm/day) $\pm$ SD	λ (day) $\pm$ SD	μ_{max} (mm/day) $\pm$ SD	λ (day) $\pm$ SD	μ_{max} (mm/day) $\pm$ SD
10	0.87	>10	NG	>10	NG	>10	NG
	0.90	>10	NG	>10	NG	>10	NG
	0.93	>10	NG	>10	NG	>10	NG
	0.95	2.89 $\pm$ 0.08 [a]	2.40 $\pm$ 0.24 [b]	2.70 $\pm$ 0.16 [a]	2.34 $\pm$ 0.13 [a]	2.87 $\pm$ 0.14 [a]	2.49 $\pm$ 0.09 [b]
	0.98	>10	5.65 $\pm$ 0.19 [a]	1.49 $\pm$ 0.05 [b]	6.03 $\pm$ 0.27 [b]	1.47 $\pm$ 0.05 [b]	6.32 $\pm$ 0.04 [a]
15	0.87	>10	NG	>10	NG	>10	NG
	0.90	>10	NG	>10	NG	>10	NG
	0.93	<0.1 [b]	1.69 $\pm$ 0.20 [c]	<0.1 [c]	1.66 $\pm$ 0.21 [c]	<0.1 [b]	1.82 $\pm$ 0.12 [c]
	0.95	0.68 $\pm$ 0.31 [a]	4.12 $\pm$ 0.13 [b]	0.26 $\pm$ 0.03 [b]	3.85 $\pm$ 0.09 [b]	0.37 $\pm$ 0.14 [a]	4.51 $\pm$ 0.07 [b]
	0.98	0.96 $\pm$ 0.27 [a]	10.56 $\pm$ 0.78 [a]	0.66 $\pm$ 0.07 [a]	10.04 $\pm$ 0.20 [a]	0.46 $\pm$ 0.10 [a]	10.11 $\pm$ 0.25 [a]
20	0.87	>10	NG	>10	NG	>10	NG
	0.90	>10	NG	>10	NG	>10	NG
	0.93	1.29 $\pm$ 0.82 [a]	3.12 $\pm$ 0.65 [c]	0.74 $\pm$ 0.28 [b]	2.98 $\pm$ 0.39 [c]	0.32 $\pm$ 0.03 [b]	3.51 $\pm$ 0.07 [c]
	0.95	1.15 $\pm$ 0.25 [a]	7.63 $\pm$ 0.28 [b]	1.36 $\pm$ 0.40 [a]	7.88 $\pm$ 0.44 [b]	0.77 $\pm$ 0.09 [a]	7.74 $\pm$ 0.26 [b]
	0.98	0.63 $\pm$ 0.09 [a]	14.14 $\pm$ 0.80 [a]	0.58 $\pm$ 0.07 [b]	13.61 $\pm$ 0.45 [a]	0.25 $\pm$ 0.01 [b]	12.94 $\pm$ 0.24 [a]
25	0.87	>10	NG	>10	NG	>10	NG
	0.90	>10	NG	>10	NG	>10	NG
	0.93	<0.1 [a]	2.62 $\pm$ 0.44 [c]	0.45 $\pm$ 0.57 [a]	3.71 $\pm$ 0.40 [c]	<0.1 [c]	3.80 $\pm$ 0.42 [c]
	0.95	0.81 $\pm$ 0.29 [a]	8.31 $\pm$ 0.50 [b]	0.64 $\pm$ 0.16 [a]	8.12 $\pm$ 0.74 [b]	0.69 $\pm$ 0.05 [a]	9.45 $\pm$ 0.58 [b]
	0.98	0.53 $\pm$ 0.10 [a]	18.98 $\pm$ 0.80 [a]	0.49 $\pm$ 0.07 [a]	18.51 $\pm$ 0.31 [a]	0.35 $\pm$ 0.16 [b]	18.38 $\pm$ 0.56 [a]
30	0.87	>10	NG	>10	NG	>10	NG
	0.90	>10	NG	>10	NG	>10	NG
	0.93	<0.1 [b]	1.27 $\pm$ 0.20 [c]	<0.1 [b]	2.22 $\pm$ 0.18 [c]	<0.1 [b]	2.20 $\pm$ 0.58 [c]
	0.95	0.76 $\pm$ 0.12 [a]	6.79 $\pm$ 0.15 [b]	0.31 $\pm$ 0.16 [a]	6.72 $\pm$ 0.23 [b]	0.87 $\pm$ 0.09 [a]	7.18 $\pm$ 0.26 [b]
	0.98	0.42 $\pm$ 0.21 [a]	12.92 $\pm$ 0.25 [a]	0.35 $\pm$ 0.03 [a]	16.99 $\pm$ 0.20 [a]	0.21 $\pm$ 0.14 [a]	16.16 $\pm$ 0.41 [a]
35	0.87	>10	NG	>10	NG	>10	NG
	0.90	>10	NG	>10	NG	>10	NG
	0.93	>10	NG	>10	NG	>10	NG
	0.95	>10	NG	>10	NG	>10	NG
	0.98	>10	NG	>10	NG	>10	NG

T: temperature; a_w: water activity; SD: standard deviation; NG: No growth observed for 10 days; >10: lag time higher than 10 days. Different letters indicate significant difference ($p < 0.05$) between a_w within every temperature and column.
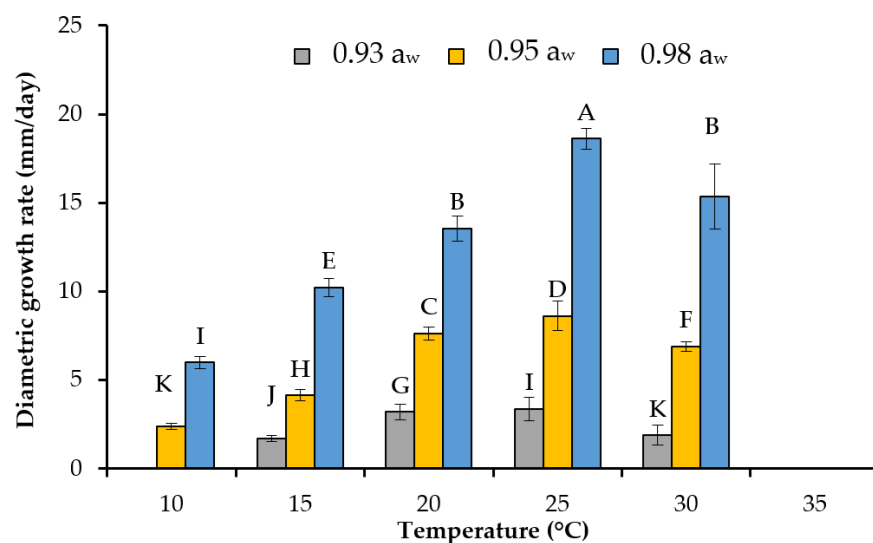

Figure 2. Effect of temperature at different steady state a_w levels on the mean growth rate (mm/day) for the mean of the three strains of *F. asiaticum* (982, 082, Ch024b) on the wheat-based media. Vertical lines represent the standard deviation, and different letters indicate a significant difference between treatments.

3.1.2. Secondary Model

Table 3 shows the cardinal values for T and a_w (minimum, maximum and optimum values) estimated with the cardinal secondary model. Models showed a good fit with R^2 = 0.93–0.99 and good RMSE = 0.48–0.69 except in the case of the strain 982 where the MSE is higher than 2. The estimated optimal (26–27 °C) and maximal T (31–32 °C) were similar for all three strains. However, the minimum T were always wrongly estimated (values below estimation were always under 0 °C). With regard to aw similar estimations were observed in the individual models as well as in that with the pooled data (0.97–0.99 a_w). The minimal a_w levels were estimated at between 0.90–0.94. The optimal fungal growth was slightly overestimated (19.9–21.4 mm/day) as the actual maximum diametric growth was 18.0 mm/day at 25 °C/0.98 a_w. The cardinal fitted model for *F. asiaticum* (strain 082) is shown Figure 3.

Table 3. Estimated parameter when the cardinal model was applied to the growth rates of the pooled data of the *F. asiaticum* strains (982, 82 and Ch024b) on a wheat-based medium.

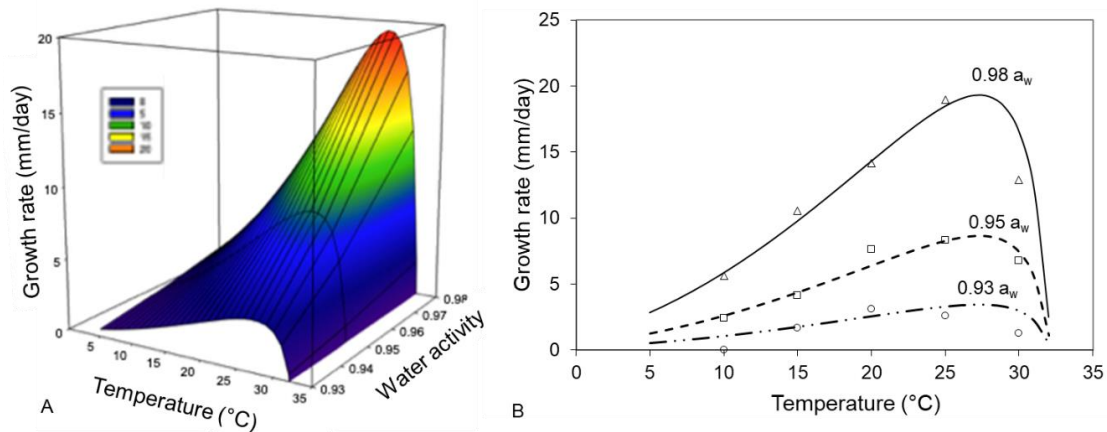| Parameters	Strains 982	82	Ch024b	Pooled Data
μ_{opt}	19.9 ± 0.97	21.38 ± 6.30	20.24 ± 0.94	20.00 ± 1.439
$a_{w\,min}$	0.94 ± 0.00	0.90 ± 0.00	0.94 ± 0.00	0.90 ± 0.002
$A_{w\,opt}$	0.97 ± 0.00	0.99 ± 0.01	0.97 ± 0.00	0.98 ± 0.003
t_{max}	31.79 ± 1.21	32.15 ± 1.27	31.4 ± 1.28	31.32 ± 0.634
t_{min}	−3.78 ± 3.48	−6.23 ± 2.12	−9.43 ± 2.57	−6.96 ± 1.444
t_{opt}	26.01 ± 0.88	27.29 ± 0.41	27.56 ± 0.59	27.22 ± 0.387
R^2	0.93	0.99	0.98	0.98
MSE	2.12	0.48	0.48	0.69

Estimated parameter ± standard deviation.

Figure 3. Cardinal fitted model of *F. asiaticum* (strain 082). (**A**) growth rate (mm/day) estimated response surface and (**B**) growth rates (mm/day) at different a_w levels (△, 0.98 a_w; □, 0.95 a_w; ○, 0.93 a_w) and fitted to the cardinal model.

3.1.3. Modelling the Growth Boundaries

The growth/no growth boundaries for all three strains were similar using the model. The probability plots of growth for interacting T and a_w after 3, 5 and 10 days for strain 082 of *F. asiaticum* are shown in Figure 4. This shows that the probability of growth in the similar environmental conditions changes over time. For example, at 0.92 a_w, the probability for growth is p = 0.5 in the range of 22–27 °C after 3 days, while in the same conditions after 5 days, this value changed to p = 0.85. In addition, the temperature range over which *F. asiaticum* can grow increased over time at 0.92 a_w with p = 0.5 occurring over a wider temperature range (12–34 °C) after 10 days growth. However, in water stress conditions for *F. asiaticum* (e.g., 0.90 a_w), the probability of growth increased slightly over time, but still remained below p = 0.30.
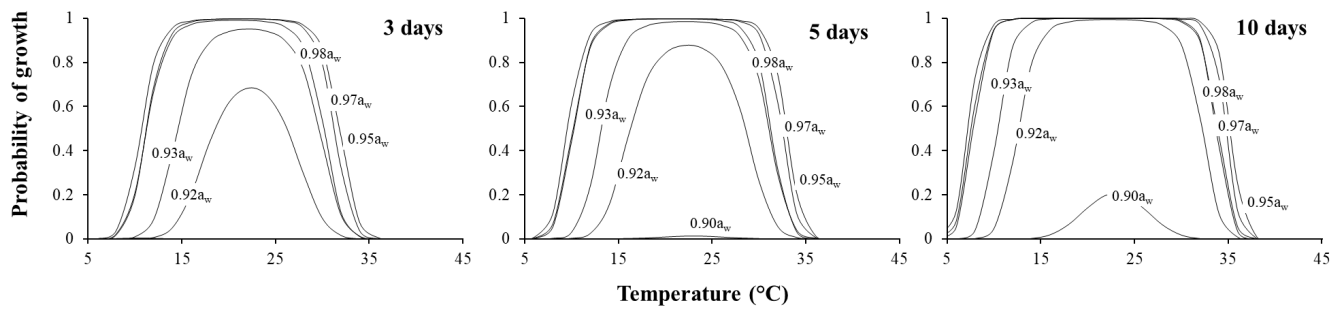
Figure 4. Estimated probability of growth of *F. asiaticum* (strain 082) under different interacting environmental conditions on a wheat-based media after 3, 5 and 10 days.

3.2. Ecophysiological Study of Mycotoxin Production

3.2.1. Mycotoxin Production

The accumulated type B trichothecenes and ZEA after 10 days growth of the strains of *F. asiaticum* was quantified (Figure 5). This showed that all the strains produced more than one mycotoxin, although 15-AcDON was only produced by *F. asiaticum* strain Ch024b at 0.98 a_w and both 25 and 30 °C (data not shown). In contrast to growth, significant differences were found between strains ($p < 0.05$) in terms of mycotoxin production. Overall, DON and ZEA were produced in higher amounts and over broader conditions than 3 and 15 AcDON and NIV. Optimal T were 25–30 °C depending on the mycotoxin, while cooler conditions restricted their production. For example, NIV and ZEA were never detected at <20 and <15 °C, respectively. Overall, trichothecenes (TCT) production was favoured by the increase in a_w and, in most cases, 0.98 a_w was the optimal condition. In contrast, the role of the a_w in ZEA production was unclear because water stress triggered toxin production under certain conditions (20–25 °C) compared to those with less restrictive a_w, but within the same T.
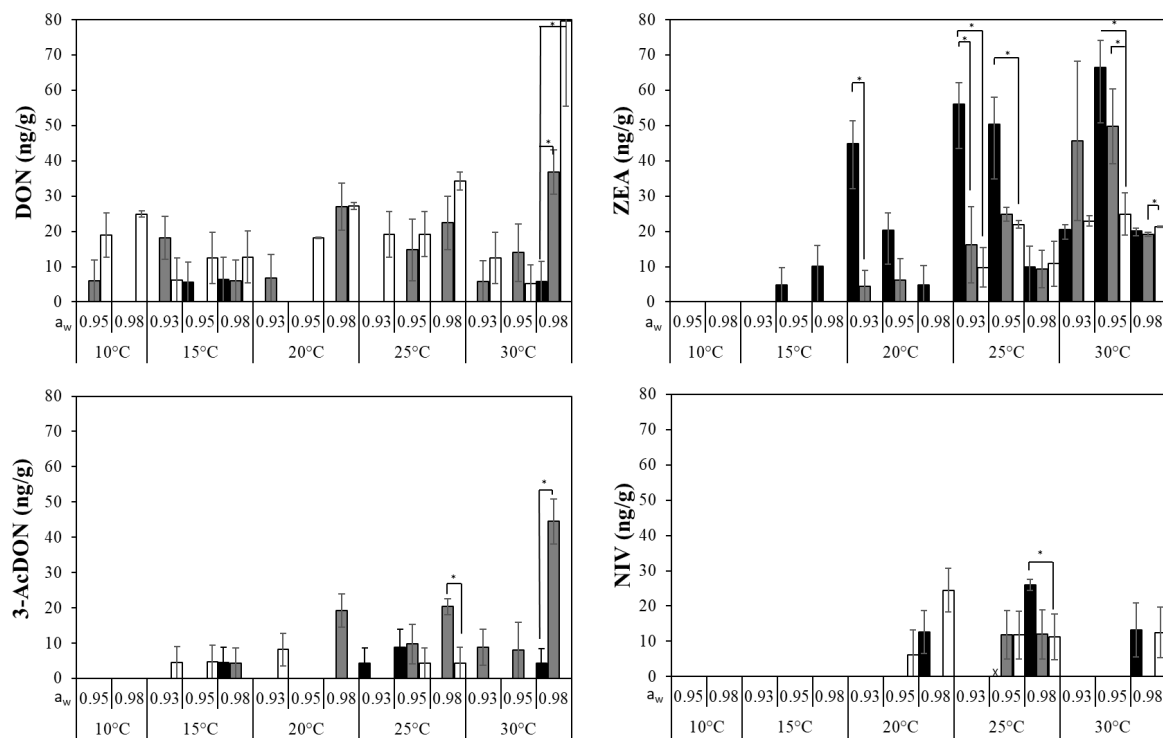

Figure 5. Deoxynivalenol (DON), 3-acetyl deoxynivalenol (3Ac-DON), zearalenone (ZEA) and nivalenol (NIV) produced by *F. asiaticum* strains (●, 982; ●, 082; ○, Ch024b) when colonizing a wheat-based medium for 10 days. Vertical bars indicate standard deviation. Asterisks indicate significant differences between strains using Wilcoxon pair comparison.

3.2.2. Modelling the Mycotoxin Production Boundaries

Probability plots were made considering the existing EU regulations for DON and ZEA in relation to production under interacting temperature x a_w conditions after 10 days for two strains of *F. asaiticum* (Figure 6). A probabilistic model for *F. asiaticum* 982 was not performed because DON was only produced at two temperatures (15, 30 °C). Different mycotoxigenic profiles were observed among both strains. Overall, environmental conditions for DON production were broader than those for ZEA. Optimal temperatures for production were between 17 and 20 °C for DON and 25 and 27 °C for ZEA. The probability of DON production increased with the a_w. In contrast, with freely available water (0.99 a_w), there was a low probability ($p = 0.4$–0.5) of production, except for strain Ch024b.
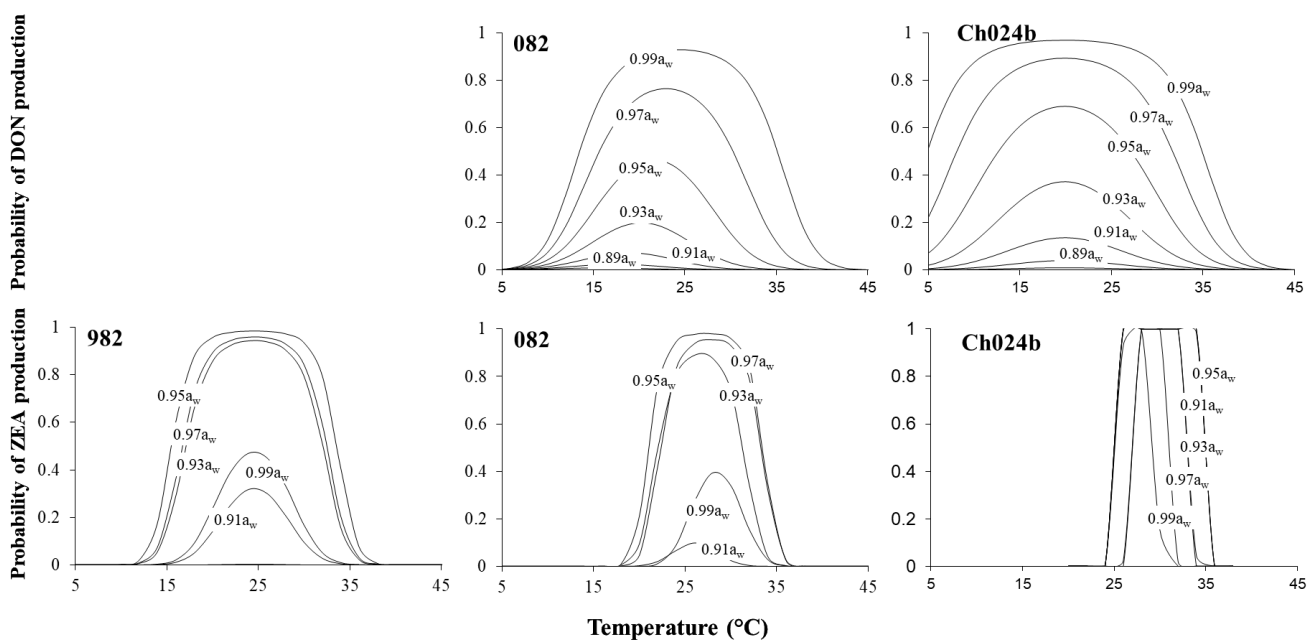

Figure 6. Estimated probability for the production of deoxynivalenol (DON) and zearalenone (ZEA) under different interacting environmental conditions by the three strains of *F. asiaticum* when colonizing a wheat-based medium after 10 days incubation.

4. Discussion

The major objective of this study was to develop models to describe the effect of interacting abiotic factors of $a_w \times T$ on the fungal growth and on DON and ZEA production by strains of *F. asiaticum* on wheat-based media for the first time. In addition, inter-species variability was assessed between three different strains of this species.

The lag phases prior to growth (λ) and the maximum growth rate (μ_{max}) were estimated with the biphasic Baranyi's function. This showed that there were no significant differences ($p > 0.05$) in these parameters between the three strains tested. Some previous studies with *F. graminearum* strains from Argentina also found very little difference in these two parameters [33]. However, the interacting abiotic factors significantly ($p > 0.05$) impacted fungal growth. *F. asiaticum* strains grew at temperatures between 10 and 30 °C. In this regard, minimum T varied from 15 °C /0.93 a_w or 10 °C/ 0.95 a_w, while growth was absent at 0.90 a_w regardless of temperature. Maximum growth (18 mm/day) was observed at 25 °C/0.98 a_w. The same range of temperatures (10–30 °C) was reported in terms of growth of other species inside the FGSC such as *F. boothii*, *F. graminearum* and *F. meridionale* [33–35]. Previously, μ_{max} for *F. graminearum sensu strito* (14 mm/day) on wheat, and *F. boothi* (14 mm/day) and *F. meridionale* (10 mm/day) on maize-based media occurred at 25 °C/0.995 a_w [33,34]. Other authors [16] found 25 °C to also be optimal for *F. graminearum* and *F. culmorum* growth but they did not examine the resilience of their strains at 30 °C. Therefore, it seems that all the FGSC have μ_{max} colonization rates over a

similar range of temperatures and perhaps also aw levels. *F. asiaticum* grew faster than other FGSC species but the experiment was performed in wheat-based media instead of wheat kernels. Higher optimal temperature (30 °C/0.98 a_w) was observed in other non-FGSC species such as *F. verticillioides* and *F. proliferatum* on maize [15]. Maximum growth rate data were fitted to cardinal model. Cardinal models estimates have biological meaning and are easy to interpret. In this study, predictions improved when the model was generated by pooling the data from the strains where the predictions were close to the observations, with the exception of the T_{min} which was predicted to be below freezing point, which is pointed out as unlikely to be an accurate estimation. Wrong T_{min} estimations has been previously reported by other authors [13,36].

Fungal colony growth is not synonymous with production of mycotoxins, even for a mycotoxigenic mould. This is because the environmental conditions may allow growth but not production of mycotoxins and toxin production may be triggered under stressing conditions for growth [37]. Therefore, in this study, the impact of the environmental conditions on ZEA, DON, 3-Ac-DON and NIV production was also assessed after 10 days. Statistical differences ($p < 0.05$) regarding the ability to produce the four mycotoxins tested were found among strains. The range of environmental conditions supporting mycotoxin production was narrower than the range supporting colony growth. For example, cold temperature inhibited production, as neither NIV and ZEA were ever detected at <20 and <15 °C, respectively, when visible growth was observed at 10 °C. It is worth mentioning that the environmental conditions suitable for producing each of the analyzed metabolites were different. NIV was only produced between 20 and 25 °C (optimal condition, 0.98 a_w/20–25 °C), 3-AcDON between 15 and 30 °C (optimal condition 0.98 a_w/30 °C for the highest produced strain), DON between 10 and 30 °C (optimal condition, 0.98 a_w/25–30 °C) and ZEA between 15 and 30 °C (optimal condition, 0.95 a_w/30 °C). Overall, the amount of trichothecenes type B (NIV, DON and 3-AcDON) produced at each temperature increased with the a_w. This was not observed in the case of ZEA where optimal production occurred even in the lowest aw supporting fungal growth, for example, 20 °C /0.93 a_w.

According to our findings, for *F. asiaticum*, previous studies reported that maximum NIV production was reached at 20–25 °C at the highest aw level tested (0.95 a_w) by *F. graminearum* [38,39] and *F. poae* [40]. However, there are discrepancies regarding the minimum temperature required for synthesizing this metabolite which had been reported for different species *F. poae* (T > 10 °C) and *F. graminearum* (T = 10 °C). Contrary to our study, 3-AcDON production by *F. graminearum* was observed at 10 °C and maximum conditions occurred at 0.95 a_w/30 °C instead of 0.98 a_w [41]. Similarly to our findings in regard to *F. asiaticum* in our study, optimal DON production occurred at 25–30 °C and the amount increased with the moisture content for *F. graminearum* [16,33,34,42] and at 20 °C for *F. boothii* [34]. The role of the a_w in the production of ZEA by *F. asiaticum* in this study was not clear. Optimal a_w in the range of 20–30 °C was 0.95 a_w, except for the strain *F. asiaticum* 982 where 0.93 a_w < 30 °C enhanced the production; this phenomenon has been previously reported in other species as *F. graminearum* in wheat [38] and in the case of *F. incarnatum* in sorghum [43]. There are maximum legal limits for DON and ZEA worldwide due to their high toxicity. For example, the EU established a limit of 750 µg/kg for DON and for 75 µg/kg for ZEA, while in China it is 1000 and 60 µg/kg, respectively, for cereals or flour intended for direct human consumption [44,45]. Most of the mycotoxin values obtained in the study were below the aforementioned values, but the experiment was conducted on wheat-based matrices for only ten days.

Finally, in this study, probabilistic models for boundary conditions of growth/toxin production were calculated. Probabilistic plots for *F. asiaticum* growth showed how the range of environmental conditions supporting the growth increased over the time and indicate a T optimal range of 15–30 °C. Probability of growth at 0.90 a_w even in the optimal T (20–26 °C according to the plot) conditions were lower than 0.2 even after 10 days. In general, our models provided solid predictions above 15 °C, however the model overestimated the growth probability in cold conditions (below 10 °C) because

real limit of growth was not observed due to lack of experiments at lower temperatures. Similar uncertainty in the prediction was observed in previous works where experimental conditions were outside the prediction model range [17]. The present model was developed with data from 10 days, however, cereals are stored for longer periods, and in some regions, it is very common to perform the drying step in an open environment under ambient conditions. Therefore, a_w could require 10 days until reaching a safety level at 14–15% moisture content (~0.87 a_w). Ideally, all models should be validated on a real matrix (wheat/barley) to assess the model's accuracy in the boundary conditions. The logistic regression model for growth of *Aspergillus* species was validated in a real matrix showing high agreement between observed and predicted probabilities [27,46]. Predicted probabilistic plots for mycotoxins depict clearly the impact of the environmental conditions in the production of DON in a wider range of temperatures compared to ZEA. The generated models indicate that ZEA accumulation in wheat can occur between 12 and 35 °C even at low a_w levels. However, growth predictions should be taken with precaution, since even at low a_w there is a high probability of toxin production. As occurred with growth, there is an overestimation in the prediction to produce DON in cold conditions by the strain *F. asiaticum* Ch024b due to the lack of boundary conditions in the experimental data. In this case, the strain was able to produce this metabolite at the lower temperature tested (10 °C). In contrast, the prediction for DON production was good in the model developed for *F. asiaticum* F082. Other authors [17] demonstrated a high percentage of concordance between predicted probability to produce type A trichothecenes (T2 + HT2) by *F. langshetiae* in oat-based media when validated with external datasets produced on media.

The present study focused only on the impact of interacting environmental conditions on growth/toxin production patterns. However, pathogens are also exposed to biotic factors in the environment. For example, in a recent study, it was found that there may be interactions between mycophagous nematodes which could influence the risk of *Fusarium* in wheat. The mathematical models developed showed that that this parameter significantly impacted *Fusarium* biomass [47].

5. Conclusions

In the present study, we developed an ecophysiological model to assess the fundamental growth and toxigenic niche of *F. asiaticum* strains for the first time. The *F. asiaticum* growth niche is similar to the other FGSC species studied by other authors. Low interspecies variability was observed regarding the fungal growth and therefore these models could be applied for controlling *F. asiaticum* colonization of wheat by their integration into a decision support system for farmers, aiming to identify pre-harvest contamination risks, but also helping to define harvesting and drying practices to minimize the post-harvest risks of contamination, with special emphasis on the drying, storage and transport steps.

Mycotoxigenic capacity of the three strains was very variable regarding the number of metabolites produced in each condition and the amount of each particular toxin. Therefore, the development of accurate prediction models for mycotoxin contamination in the food chain remains challenging.

Author Contributions: E.G.-C.: Conceptualization, Methodology, Formal analysis, Writing—original draft, Writing—review & Supervision. C.V.-V.: Conceptualization, Methodology, Formal analysis, Writing—review & Supervision. I.Ó.-J.: Investigation & methodology. R.L.: Methodology. N.M.: Writing—review & editing, Funding acquisition. All authors have read and agreed to the published version of the manuscript.

References

1. FAO. FAOSTAT. Available online: https://www.fao.org/faostat/en/#home (accessed on 2 October 2022).
2. Magan, N.; Garcia-Cela, E.; Verheecke-Vaessen, C.; Medina, A. Advances in post-harvest detection and control of fungal contamination of cereals. In *Advances in Postharvest Management of Cereals and Grains*; Burleigh Dodds Science Publishing: London, UK, 2020; pp. 339–362. ISBN 9781003047988.
3. Al-Hazmi, N.A.; Gomaa, M.N. Alteration of fungal growth and toxigenicity due to the protective effect of cereal coats. *Food Control* **2012**, *28*, 299–303. [CrossRef]
4. Vaughan, M.; Backhouse, D.; Del Ponte, E.M. Climate change impacts on the ecology of *Fusarium graminearum* species complex and susceptibility of wheat to Fusarium head blight: A review. *World Mycotoxin J.* **2016**, *9*, 685–700. [CrossRef]
5. Aoki, T.; Ward, T.J.; Kistler, H.C.; Odonnell, K. Systematics, Phylogeny and Trichothecene Mycotoxin Potential of Fusarium Head Blight Cereal Pathogens. *JSM Mycotoxins* **2012**, *62*, 91–102. [CrossRef]
6. van der Lee, T.; Zhang, H.; van Diepeningen, A.; Waalwijk, C. Biogeography of Fusarium graminearum species complex and chemotypes: A review. *Food Addit. Contam. Part A. Chem. Anal. Control Expo. Risk Assess.* **2015**, *32*, 453–460. [CrossRef] [PubMed]
7. Jennings, P. Fusarium Mycotoxins: Chemistry, Genetics and Biology—by Anne E. Desjardins. *Plant Pathol.* **2007**, *56*, 337. [CrossRef]
8. Mostrom, M. Trichothecenes and zearalenone. In *Reproductive and Developmental Toxicology*; Academic Press: Cambridge, MA, USA, 2011; pp. 739–751. [CrossRef]
9. Magan, N.; Aldred, D.; Mylona, K.; Lambert, R.J.W. Limiting mycotoxins in stored wheat. *Food Addit. Contam.-Part A* **2010**, *27*, 644–650. [CrossRef]
10. Magan, N.; Aldred, D. Post-harvest control strategies: Minimizing mycotoxins in the food chain. *Int. J. Food Microbiol.* **2007**, *119*, 131–139. [CrossRef]
11. Baranyi, J.; Gibson, A.M.; Pitt, J.I.; Eyles, M.J.; Roberts, T.A. Predictive models as means of measuring the relatedness of some Aspergillus species. *Food Microbiol.* **1997**, *14*, 347–351. [CrossRef]
12. Marín, S.; Colom, C.; Sanchis, V.; Ramos, A.J. Modelling of growth of aflatoxigenic *A. flavus* isolates from red chilli powder as a function of water availability. *Int. J. Food Microbiol.* **2009**, *128*, 491–496. [CrossRef]
13. Astoreca, A.; Vaamonde, G.; Dalcero, A.; Ramos, A.J.; Marín, S. Modelling the effect of temperature and water activity of *Aspergillus flavus* isolates from corn. *Int. J. Food Microbiol.* **2012**, *156*, 60–67. [CrossRef]
14. García-Cela, E.; Crespo-Sempere, A.; Ramos, A.J.; Sanchis, V.; Marin, S. Ecophysiological characterization of *Aspergillus carbonarius, Aspergillus tubingensis* and *Aspergillus* niger isolated from grapes in Spanish vineyards. *Int. J. Food Microbiol.* **2014**, *173*, 89–98. [CrossRef] [PubMed]
15. Samapundo, S.; Devliehgere, F.; De Meulenaer, B.; Debevere, J. Effect of water activity and temperature on growth and the relationship between fumonisin production and the radial growth of *Fusarium verticillioides* and *Fusarium proliferatum* on corn. *J. Food Prot.* **2005**, *68*, 1054–1059. [CrossRef] [PubMed]
16. Hope, R.; Aldred, D.; Magan, N. Comparison of environmental profiles for growth and deoxynivalenol production by *Fusarium culmorum* and *F. graminearum* on wheat grain. *Lett. Appl. Microbiol.* **2005**, *40*, 295–300. [CrossRef] [PubMed]
17. Verheecke-Vaessen, C.; Garcia-Cela, E.; Lopez-Prieto, A.; Osk Jonsdottir, I.; Medina, A.; Magan, N. Water and temperature relations of *Fusarium langsethiae* strains and modelling of growth and T-2 and HT-2 mycotoxin production on oat-based matrices. *Int. J. Food Microbiol.* **2021**, *348*, 109203. [CrossRef]
18. Pei, P.; Xiong, K.; Wang, X.; Sun, B.; Zhao, Z.; Zhang, X.; Yu, J. Predictive growth kinetic parameters and modelled probabilities of deoxynivalenol production by *Fusarium graminearum* on wheat during simulated storing conditions. *J. Appl. Microbiol.* **2022**, *133*, 349–361. [CrossRef]
19. Yang, L.; Van Der Lee, T.; Yang, X.; Yu, D.; Waalwijk, C. *Fusarium* populations on Chinese barley show a dramatic gradient in mycotoxin profiles. *Phytopathology* **2008**, *98*, 719–727. [CrossRef]
20. Zhang, H.; Zhang, Z.; Van Der Lee, T.; Chen, W.Q.; Xu, J.; Xu, J.S.; Yang, L.; Yu, D.; Waalwijk, C.; Feng, J. Population genetic analyses of *Fusarium asiaticum* populations from barley suggest a recent shift favoring 3ADON producers in southern China. *Phytopathology* **2010**, *100*, 328–336. [CrossRef]

21. Del Ponte, E.M.; Spolti, P.; Ward, T.J.; Gomes, L.B.; Nicolli, C.P.; Kuhnem, P.R.; Silva, C.N.; Tessmann, D.J. Regional and field-specific factors affect the composition of fusarium head blight pathogens in subtropical no-till wheat agroecosystem of Brazil. *Phytopathology* **2015**, *105*, 246–254. [CrossRef]

22. Desjardins, A.E.; Proctor, R.H. Genetic diversity and trichothecene chemotypes of the Fusarium graminearum clade isolated from maize in Nepal and identification of a putative new lineage. *Fungal Biol.* **2011**, *115*, 38–48. [CrossRef]

23. Gale, L.R.; Harrison, S.A.; Ward, T.J.; O'Donnell, K.; Milus, E.A.; Gale, S.W.; Kistler, H.C. Nivalenol-type populations of Fusarium graminearum and F. asiaticum are prevalent on wheat in southern Louisiana. *Phytopathology* **2011**, *101*, 124–134. [CrossRef]

24. Gomes, L.B.; Ward, T.J.; Badiale-Furlong, E.; Del Ponte, E.M. Species composition, toxigenic potential and pathogenicity of Fusarium graminearum species complex isolates from southern Brazilian rice. *Plant Pathol.* **2015**, *64*, 980–987. [CrossRef]

25. Suga, H.; Karugia, G.W.; Ward, T.; Gale, L.R.; Tomimura, K.; Nakajima, T.; Miyasaka, A.; Koizumi, S.; Kageyama, K.; Hyakumachi, M. Molecular Characterization of the Fusarium graminearum Species Complex in Japan. *Am. Phytopath. Soc.* **2008**, *98*, 159. [CrossRef] [PubMed]

26. Backhouse, D. Global distribution of *Fusarium graminearum, F. asiaticum* and *F. boothii* from wheat in relation to climate. *Eur. J. Plant Pathol.* **2014**, *139*, 161–173. [CrossRef]

27. Garcia, D.; Ramos, A.J.; Sanchis, V.; Marín, S. Modelling the effect of temperature and water activity in the growth boundaries of *Aspergillus ochraceus* and *Aspergillus parasiticus*. *Food Microbiol.* **2011**, *28*, 406–417. [CrossRef]

28. Zwietering, M.H.; De Wit, J.C.; Notermans, S. Application-of predictive microbiology to estimate the number of *Bacillus cereus* in pasteurised milk at the point of consumption. *Int. J. Food Microbiol.* **1996**, *30*, 55–70. [CrossRef]

29. Rosso, L.; Lobry, J.R.; Bajard, S.; Flandrois, J.P. Convenient model to describe the combined effects of temperature and pH on microbial growth. *Appl. Environ. Microbiol.* **1995**, *61*, 610–616. [CrossRef]

30. Sautour, M.; Dantigny, P.; Divies, C.; Bensoussan, M. A temperature-type model for describing the relationship between fungal growth and water activity. *Int. J. Food Microbiol.* **2001**, *67*, 63–69. [CrossRef]

31. Isidro-Sánchez, J.; D'Arcy Cusack, K.; Verheecke-Vaessen, C.; Kahla, A.; Bekele, W.; Doohan, F.; Magan, N.; Medina, A. Genome-wide association mapping of *Fusarium langsethiae* infection and mycotoxin accumulation in oat (*Avena sativa* L.). *Plant Genome* **2020**, *13*, e20023. [CrossRef]

32. Malachová, A.; Sulyok, M.; Beltrán, E.; Berthiller, F.; Krska, R. Optimization and validation of a quantitative liquid chromatography-tandem mass spectrometric method covering 295 bacterial and fungal metabolites including all regulated mycotoxins in four model food matrices. *J. Chromatogr. A* **2014**, *1362*, 145–156. [CrossRef]

33. Ramirez, M.L.; Chulze, S.; Magan, N. Temperature and water activity effects on growth and temporal deoxynivalenol production by two Argentinean strains of *Fusarium graminearum* on irradiated wheat grain. *Int. J. Food Microbiol.* **2006**, *106*, 291–296. [CrossRef]

34. Belizán, M.M.; Gomez, A.D.L.A.; Baptista, Z.P.T.; Jimenez, C.M.; Matías, M.D.H.S.; Catalán, C.A.; Sampietro, D.A. Influence of water activity and temperature on growth and production of trichothecenes by *Fusarium graminearum* sensu stricto and related species in maize grains. *Int. J. Food Microbiol.* **2019**, *305*, 108242. [CrossRef] [PubMed]

35. Brennan, J.M.; Fagan, B.; Van Maanen, A.; Cooke, B.M.; Doohan, F.M. Studies on in vitro growth and pathogenicity of European Fusarium fungi. *Eur. J. Plant Pathol.* **2003**, *109*, 577–587. [CrossRef]

36. Ratkowsky, D.A.; Olley, J.; Ross, T. Unifying temperature effects on the growth rate of bacteria and the stability of globular proteins. *J. Theor. Biol.* **2005**, *233*, 351–362. [CrossRef] [PubMed]

37. Garcia, D.; Ramos, A.J.; Sanchis, V.; Marín, S. Predicting mycotoxins in foods: A review. *Food Microbiol.* **2009**, *26*, 757–769. [CrossRef]

38. Garcia-Cela, E.; Kiaitsi, E.; Medina, A.; Sulyok, M.; Krska, R.; Magan, N. Interacting Environmental Stress Factors Affects Targeted Metabolomic Profiles in Stored Natural Wheat and That Inoculated with F. graminearum. *Toxins* **2018**, *10*, 56. [CrossRef]

39. Llorens, A.; Mateo, R.; Hinojo, M.J.; Valle-Algarra, F.M.; Jiménez, M. Influence of environmental factors on the biosynthesis of type B trichothecenes by isolates of Fusarium spp. from Spanish crops. *Int. J. Food Microbiol.* **2004**, *94*, 43–54. [CrossRef]

40. Nazari, L.; Pattori, E.; Manstretta, V.; Terzi, V.; Morcia, C.; Somma, S.; Moretti, A.; Ritieni, A.; Rossi, V. Effect of temperature on growth, wheat head infection, and nivalenol production by *Fusarium poae*. *Food Microbiol.* **2018**, *76*, 83–90. [CrossRef]

41. Ramírez Albuquerque, D.; Patriarca, A.; Fernández Pinto, V. Water activity influence on the simultaneous production of DON, 3-ADON and 15-ADON by a strain of Fusarium graminearum ss of 15-ADON genotype. *Int. J. Food Microbiol.* **2022**, *373*, 109721. [CrossRef]

42. Garcia-Cela, E.; Kiaitsi, E.; Sulyok, M.; Medina, A.; Magan, N. Fusarium graminearum in Stored Wheat: Use of CO2 Production to Quantify Dry Matter Losses and Relate This to Relative Risks of Zearalenone Contamination under Interacting Environmental Conditions. *Toxins* **2018**, *10*, 86. [CrossRef]

43. Lahouar, A.; Marin, S.; Crespo-Sempere, A.; Saïd, S.; Sanchis, V. Influence of temperature, water activity and incubation time on fungal growth and production of ochratoxin A and zearalenone by toxigenic *Aspergillus tubingensis* and *Fusarium incarnatum* isolates in sorghum seeds. *Int. J. Food Microbiol.* **2017**, *242*, 53–60. [CrossRef]

44. European Commission Commission Regulation (EC). No 1881/2006 of 19 December 2006 setting maximumlevels for certain contaminants in foodstuffs. *Off. J. Eur. Commun.* **2006**, *L364*, 5–24.

45. China Food and Drug Administration (CFDA). *GB 2761-2017 National Standard for Food Safety—Limits of Mycotoxins in Food*; National Health and Family Planning Commmission of People´s Republic of China: Beijing, China, 2017.

46. Marín, S.; Hodžić, I.; Ramos, A.J.; Sanchis, V. Predicting the growth/no-growth boundary and ochratoxin A production by *Aspergillus carbonarius* in pistachio nuts. *Food Microbiol.* **2008**, *25*, 683–689. [CrossRef] [PubMed]

47. Goncharov, A.A.; Gorbatova, A.S.; Sidorova, A.A.; Tiunov, A.V.; Bocharov, G.A. Mathematical modelling of the interaction of winter wheat (*Triticum aestivum*) and *Fusarium* species (*Fusarium* spp.). *Ecol. Modell.* **2022**, *465*, 109856. [CrossRef]